



Room-temperature multiferroic behavior in layer-structured Aurivillius phase ceramics

Cite as: Appl. Phys. Lett. **117**, 052903 (2020); <https://doi.org/10.1063/5.0017781>

Submitted: 09 June 2020 . Accepted: 25 July 2020 . Published Online: 07 August 2020

Zheng Li, Vladimir Koval , Amit Mahajan, Zhipeng Gao, Carlo Vecchini, Mark Stewart, Markys G. Cain , Kun Tao, Chenglong Jia , Giuseppe Viola, and Haixue Yan 



View Online



Export Citation



CrossMark

ARTICLES YOU MAY BE INTERESTED IN

[Intrinsic piezoelectricity in \(K,Na\)NbO₃-based lead-free single crystal: Piezoelectric anisotropy and its evolution with temperature](#)

Applied Physics Letters **117**, 052904 (2020); <https://doi.org/10.1063/5.0012124>

[Current-induced bulk magnetization of a chiral crystal CrNb₃S₆](#)

Applied Physics Letters **117**, 052408 (2020); <https://doi.org/10.1063/5.0017882>

[Magnetic transition behavior and large topological Hall effect in hexagonal Mn_{2-x}Fe_{1+x}Sn \(x = 0.1\) magnet](#)

Applied Physics Letters **117**, 052407 (2020); <https://doi.org/10.1063/5.0011570>



Measure Ready
FastHall™ Station

The highest performance tablet system...
for van der Pauw and Hall bar samples

[Learn more](#)

Lake Shore
CRYOTRONICS

Room-temperature multiferroic behavior in layer-structured Aurivillius phase ceramics

Cite as: Appl. Phys. Lett. **117**, 052903 (2020); doi: [10.1063/5.0017781](https://doi.org/10.1063/5.0017781)

Submitted: 9 June 2020 · Accepted: 25 July 2020 ·

Published Online: 7 August 2020 · Corrected: 11 August 2020



View Online



Export Citation



CrossMark

Zheng Li,¹ Vladimir Koval,² Amit Mahajan,³ Zhipeng Gao,⁴ Carlo Vecchini,⁵ Mark Stewart,⁵ Markys G. Cain,⁶ Kun Tao,⁷ Chenglong Jia,^{7,a)} Giuseppe Viola,³ and Haixue Yan^{3,b)} 

AFFILIATIONS

¹Gemological Institute, China University of Geosciences, Wuhan 430074, China

²Institute of Materials Research, Slovak Academy of Sciences, Watsonova 47, Kosice 04001, Slovakia

³School of Engineering and Materials Science, Queen Mary, University of London, London E1 4NS, United Kingdom

⁴National Key Laboratory of Shock Wave and Detonation Physics Institute of Fluid Physics, China Academy of Engineering Physics, Mianyang 621900, China

⁵National Physical Laboratory, Hampton Road, Teddington TW11 0LW, United Kingdom

⁶Electrosiences Ltd, Farnham, Surrey GU9 9QT, United Kingdom

⁷School of Physical Science and Technology, Lanzhou University, Lanzhou 730000, China

a) Email: cljia@lzu.edu.cn

b) Author to whom correspondence should be addressed: h.x.yan@qmul.ac.uk

ABSTRACT

M

Layer-structured Aurivillius phase ceramics ($B_5F_2O_{15}$) exhibit multiferroic behavior at room temperature. The multiferroic behavior is attributed to the presence of F^{3+} and C^{3+} ions in the Aurivillius phase. The F^{3+} and C^{3+} ions are located at the B sites of the Aurivillius phase, which leads to the formation of $B_5F_2O_{15}$ and $B_5C_2O_{15}$ phases. The $B_5F_2O_{15}$ phase is a ferroelectric (FE) phase, while the $B_5C_2O_{15}$ phase is a ferromagnetic (FM) phase. The coexistence of FE and FM phases in the Aurivillius phase leads to multiferroic behavior. The multiferroic behavior is characterized by the presence of a magnetic field-induced electric polarization (ME) effect. The ME effect is observed in the Aurivillius phase at room temperature. The ME effect is attributed to the presence of F^{3+} and C^{3+} ions in the Aurivillius phase. The ME effect is characterized by the presence of a magnetic field-induced electric polarization (ME) effect. The ME effect is observed in the Aurivillius phase at room temperature. The ME effect is attributed to the presence of F^{3+} and C^{3+} ions in the Aurivillius phase.

Published under license by AIP Publishing. <https://doi.org/10.1063/5.0017781>

M

(FM)

(FE)

$(= 4)$
 $(= 5)$

$B_5F_2O_{15}$ ($= 4$) $B_6F_2O_{18}$
 B_4O_{12}

^{1,4} H

$B_5F_2O_{15}$

$B_6F_2O_{18}$

FE FM

^{12,13} B

$B_5F_2O_{15}$

⁵

$(B_2O_2)^{2+}$

$(A_{-1}B_{+1}O_3)^{2-}$

$(A_{-1}B_{+1}O_3)^{2-}$

A

$(= 4)$

$(= 5)$

^{14,15} H

$B_6F_2O_{18}$

$(= 5)$

$B_5F_2O_{15}$

B-

$B_5F_2O_{15}$

^{7,11}

A

$B_{5.25}Li_{0.75}FeC_{18}O_{18}$
 $(BLFC)_{P-L}$
 F, A, C, D
 a, b, P
 A
 $in situ$
 I, H, O, K
 $A, BLFC$
 $BLFC$
 P
 $F, 1$
 $(BLFC)$
 $B2cb$
 A
 A_{21}
 $A_{21}am$
 $B2cb$
 $a = 5.4530(2) \text{ \AA}, b = 5.4427(1) \text{ \AA}, c = 50.670(2) \text{ \AA}$
 $A_{21}am$
 $a = 5.4651(6) \text{ \AA}, c = 41.487(2) \text{ \AA}$
 F, P

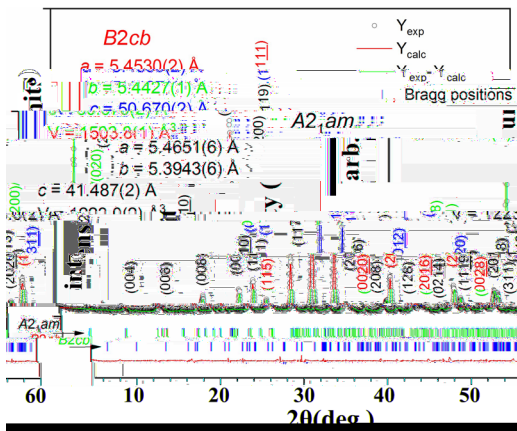


FIG. 1. XRD patterns of B2cb and A21am phases.

$BLFC$
 $= 4, = 5$
 A, N
 $BLFC$
 $F, 1$
 $EM (a-b)$
 P, M
 $F, 1$
 1.4%
 D, ED
 $(F, 2)$
 $1)$
 $F, C, O,$
 $C_2F_2O_4$
 A
 $B_{5.25}Li_{0.75}FeC_{18}O_{18}$
 $F, 2()$
 $BLFC$
 P
 $(50, 70, 100,$
 $300, 500 \text{ H})$
 1060 K
 $FE T$
 $BLFC, H$
 $B_{6.5}F_{0.5}C_{0.5}O_{15}$
 $(973 \text{ K}), F, 2()$
 $P-E, I-E$
 $BLFC$
 P
 $I-E$
 $21, 22$
 $BLFC$
 $F, 10 \mu C/$
 $2()$
 (FC)
 200 O
 $BLFC$
 $BLFC$

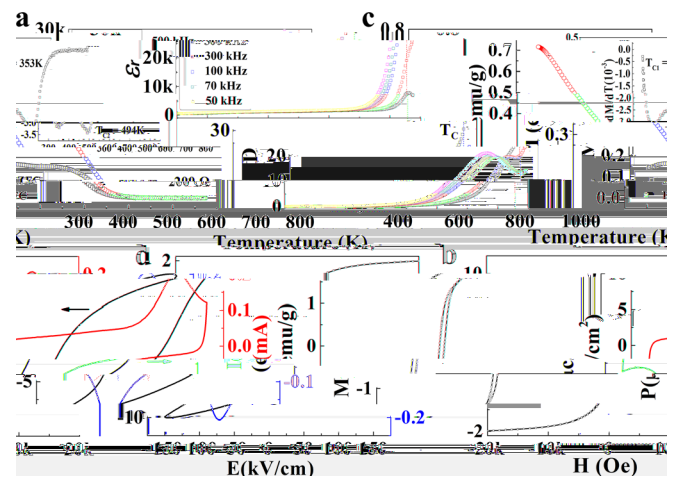


FIG. 2. (a) Impedance spectra of B2cb at various frequencies. (b) Temperature dependence of the real part of impedance Z' for B2cb. (c) Temperature dependence of the imaginary part of impedance Z'' for B2cb. (d) Temperature dependence of the real part of impedance Z' for A21am. (e) Temperature dependence of the imaginary part of impedance Z'' for A21am. (f) Temperature dependence of the real part of impedance Z' for BLFC. (g) Temperature dependence of the imaginary part of impedance Z'' for BLFC. (h) Temperature dependence of the real part of impedance Z' for BLFC. (i) Temperature dependence of the imaginary part of impedance Z'' for BLFC.

~ 494 K
 M/μ_B ,
 $B_6F_2C_{18}O_{18}$ (526 K).²³
 BLFC
 $F^{3+} O F^{3+}, C^{3+} O C^{3+}, F^{3+} O C^{3+}$ ().²⁴
 ED
 ~ 353 K
 FC
 $C_2F_4O_4$ (460 K)
 $(M) C_2F_4O_4$ 16,25
 $16.235 / 0.22, 0.32 / 1.4$ %
 $C_2F_4O_4$
 $M = 1.85 / F = 2(1.1)$
 $M H$
 ~ 425 K 1.58 / 0.27 / ED
 $BLFC$
 $F^{3+} O C^{3+}$
 (DF) *ab initio*
 $(A P) F C$
 $\mu_F = 2, \mu_C = 3$
 (GGA)+
 $BLFC$
 $F = 3(1), F^{3+} C^{3+} (3.1, 2.1 \mu_B)$
 $(0.1 \mu_B) F O_6 C O_6$
 F / C
 F
 $F^{3+} C^{3+}$
 (\dots)
 $E_{FM} - E_{AFM} = -144.1$
 H 43.5 (504.6 K) (FM)
 FC/FC $F = 2(1)$
 $a b$
 010
 $BLFC$ $F = 4$
 I

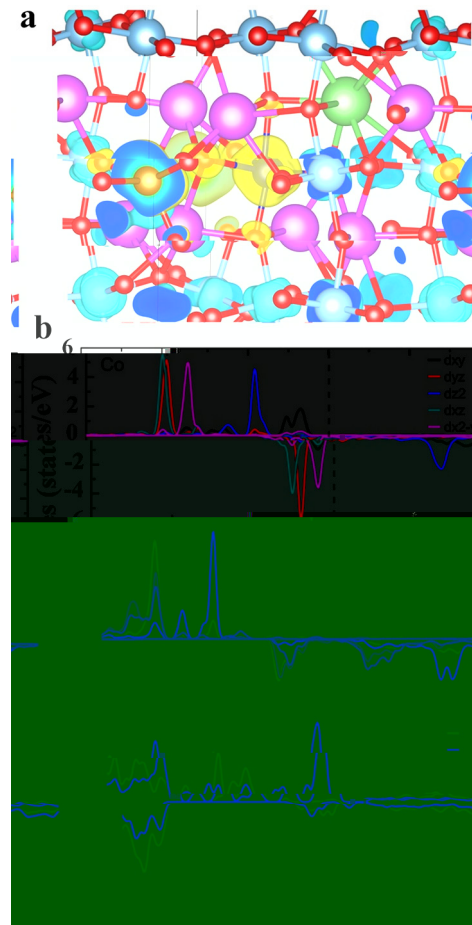


FIG. 3. (a) Crystal structure of BLFC showing layers of fluorine (red), carbon (blue), and oxygen (green) atoms. (b) Density of states (DOS) plot showing energy levels (states/eV) versus energy (eV) for different orbitals (dxy, dx2-y2, dz2, dxz, dyz).

$(2^- < H < 5^-)$,
 $M H$ $F = 2(1)$ $3.F$
 $BLFC$ P $F M$
 PFM $BLFC$ 399 O
 $5(1).A$ F

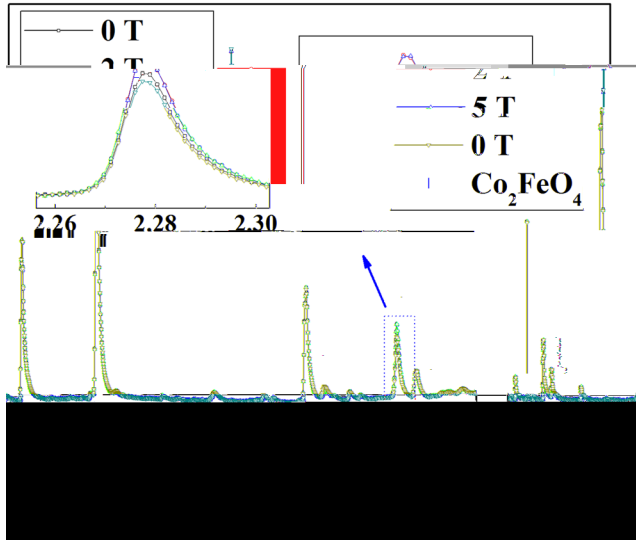


FIG. 4. XRD patterns of Co_2FeO_4 at 0 T and 5 T. The inset shows a zoomed-in view of the 2.26–2.30 degree range.

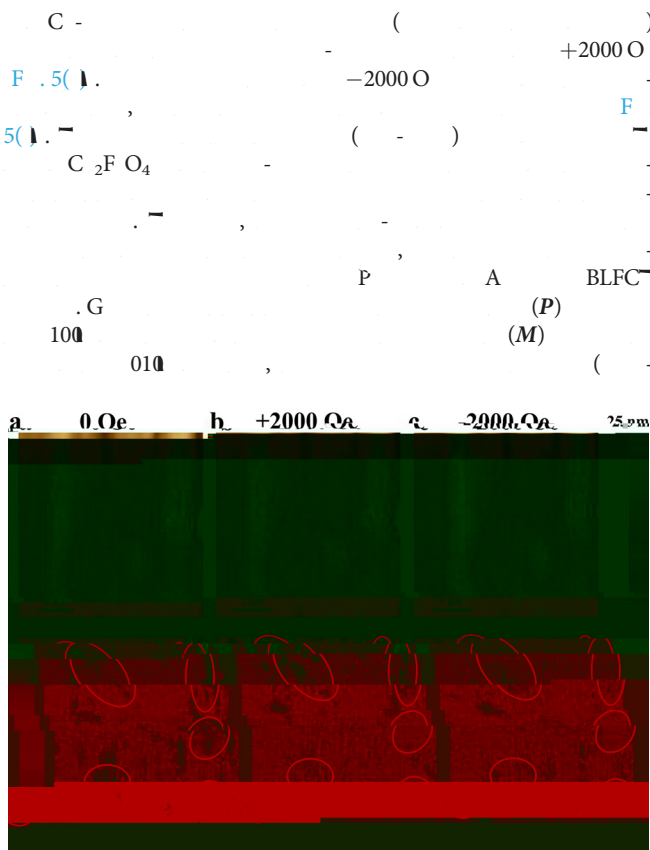


FIG. 5. MFM images of Co_2FeO_4 at 0 Oe, +2000 Oe, and -2000 Oe. The images show magnetic domains with red circles highlighting specific features. The scale bar is 25.0 nm.

$T = P \times M$
 BLFC^-
 BLFC^-
 $\text{F}^{3+} \text{O} \text{F}^{3+}$
 $\text{C}^{3+} \text{O} \text{C}^{3+}, \text{F}^{3+} \text{O} \text{C}^{3+}$
 C / F
 EM^- (ED) BLFC^-
 $\text{D} \cdot \text{M}, \text{P} \text{D} \cdot \text{K}$
 $\text{D} \text{I} \text{H} \text{I} \text{I} \text{N}$
 $\text{D}, \text{O}, \text{K}$
 $\text{A} \text{E} \text{D} \text{F}$
 $\text{G} \text{A} \text{A} \text{G} \text{N} \cdot \text{K}2015-0602006, \text{N} \text{FC} \text{G}$
 $\text{N} \cdot 11474138 \text{11834005}$
 $\text{E} \text{M} \text{P} \text{EM} \text{P}$
 $\text{IND54} \text{N} \text{EM} \text{P}$
 $\text{EM} \text{P} \text{E} \text{AME} \text{E}$

DATA AVAILABILITY

REFERENCES

1. E. N. D. M., J. F., *N* **442**, 759 (2006).
2. N. A., *N. M.* **6**, 21 (2007).
3. J. M., J. H., L., C., *N. A. M.* **23**, 1062 (2011).
4. L. F. H., O. C., J. B., J. L., C. H., H., H., O. G., D. C. L., H., K., A. J. B., *A. F. M.* **26**, 2111 (2016).
5. N. A. H., *J. P. C. B* **104**, 6694 (2000).
6. B. A., M. : II.
7. $\text{B}_4\text{O}_3\text{O}_{12}$, A. K. **1**(58), 499–512 (1949).
8. A., G. K., M. M. K., *J. P. C. M.* **11**, 3335 (1999).
9. N. P., G. K., *M. E. B* **108**, 194 (2004).
10. L. K., M., M., A. A., N. D., N. P., E. P., D. J., *J. A. C.* **96**, 2339 (2013).
11. L., J. M., G., G., K., A. M., L., C. J., C. N., H., *D.* **45**, 14049 (2016).
12. J. F., *NPGA M.* **5**, 72 (2013).
13. A., B. C. E., *P. B* **90**, 214109 (2014).
14. J. B. L., P. H., G. H., G., L., J. L., J. C., J. K. L., *A. P. L.* **96**, 222903 (2010).
15. M., C., L., *A. P. L.* **95**, 082901 (2009).
16. L., J., L., J. D., *A. P. L.* **101**, 122402 (2012).

- ¹⁶M. P. , P. C. , M. B. , A. P. B. , J. P. H. , K. , L. K. , M. P. , C. , H. K. , A. J. B. , *J. A. P.* **112**, 073919 (2012).
- ¹⁷J. L. , H. , M. J. , K. , P. , *J. A. P.* **102**, 104107 (2007).
- ¹⁸M. G. C. , *Characterisation of Ferroelectric Bulk Materials and Thin Films* (, 2014), .2.
- ¹⁹.L., K. , J. M. , G. , K. , C. J. , G. , H. , A. M. , J. C. , M. C. , I. A. , C. N. , C. J. , H. , *J. M. C. C.* **6**, 2733 (2018).
- ²⁰. K. , I. , G. , M. , C. J. , H. , *J. P. C.* **122**, 15733 (2018).
- ²¹L. J. , F. L. , *J. A. C.* **97**, 1 (2014).
- ²²H. , F. I. , G. , H. N. , H. , J. , G. , M. J. , *J. A. D.* **1**, 107 (2011).
- ²³J. , L. , L. , J. D. , A. , *P. L.* **101**, 012402 (2012).
- ²⁴B. , J. , J. C. , L. , J. D. , A. , *P. L.* **104**, 062413 (2014).
- ²⁵L. P. M. , N. B. , *J. M. C. C.* **11**, 719 (2009).